Urban forest microclimates across temperate Europe are shaped by deep edge effects and forest structure.

Karen De Pauw[1], Leen Depauw[1], Kim Calders[2], Steven Caluwaerts[3,4], Sara A.O. Cousins[5], Emiel De Lombaerde[1], Martin Diekmann[6], David Frey[7], Jonathan Lenoir[8], Camille Meeussen[1], Anna Orczewska[9], Jan Plue[10], Fabien Spicher[8], Florian Zellweger[11], Pieter Vangansbeke[1], Kris Verheyen[1] and Pieter De Frenne[1]

1. Forest & Nature Lab, Department of Environment, Faculty of Bioscience Engineering, Ghent University, Geraardsbergsesteenweg 267, 9090, Melle-Gontrode, Belgium
2. CAVElab – Computational & Applied Vegetation Ecology, Department of Environment, Ghent University, Belgium
3. Atmospheric Physics Group, Department of Physics and astronomy, Faculty of Sciences, Ghent University, Krijgslaan 281, 9000 Ghent
4. Department Meteorological and Climatological Research, Royal Meteorological Institute of Belgium, Avenue Circulaire 3, 1180, Brussels, Belgium
5. Landscapes, Environment and Geomatics, Department of Physical Geography, Stockholm University, Svante Arrhenius väg 8, 106 91, Stockholm, Sweden
6. Vegetation Ecology and Conservation Biology, Institute of Ecology, FB2, University of Bremen, Bremen, Germany
7. Al Ciòs Consulenze ambientali, Via Cantonale 79, 6818 Melano, Switzerland"
8. UR "Ecologie et Dynamique des Systèmes Anthropisés" (EDYSAN, UMR 7058 CNRS-UPJV), Universiteé de Picardie Jules Verne, rue des Louvels 1, Amiens Cedex, 80037, France
9. Institute of Biology, Biotechnology and Environmental Protection, Faculty of Natural Sciences, University of Silesia, Katowice, Poland
10. Department of Urban and Rural Development; SLU Swedish Biodiversity Centre (CBM). Inst.för stad och land, 75007 Uppsala
11. Swiss Federal Research Institute for Forest, Snow and Landscape Research WSL, Birmensdorf 8903, Switzerland

Contact information:
Karen.depauw@ugent.be; +32 470 04 46 97

Karen De Pauw https://orcid.org/0000-0001-8369-2679
Leen Depauw https://orcid.org/0000-0001-5703-6811
Kim Calders https://orcid.org/0000-0002-4562-2538
Steven Caluwaerts https://orcid.org/0000-0001-7456-3891
Sara A.O. Cousins https://orcid.org/0000-0003-2656-2645
Emiel De Lombaerde https://orcid.org/0000-0002-0050-2735
Martin Diekmann https://orcid.org/0000-0001-8482-0679
David Frey https://orcid.org/0000-0002-4603-0438
Jonathan Lenoir https://orcid.org/0000-0003-0638-9582
Camille Meeussen https://orcid.org/0000-0002-5869-4936
Anna Orczewska https://orcid.org/0000-0002-7924-9794
Jan Plue https://orcid.org/0000-0002-6999-669X
Fabien Spicher https://orcid.org/0000-0002-9999-955X

Florian Zellweger https://orcid.org/0000-0003-1265-9147
Pieter Vangansbeke https://orcid.org/0000-0002-6356-2858
Kris Verheyen https://orcid.org/0000-0002-2067-9108
Pieter De Frenne https://orcid.org/0000-0002-8613-0943

Abstract

The urban heat island (UHI) causes strong warming of cities and their urban forests worldwide. Especially urban forest edges are strongly exposed to the UHI effect, which could impact urban forest biodiversity and functioning. However, it is not known to what extent the UHI effect alters edge-to-interior microclimatic gradients within urban forests and whether this depends on the forests' structure.

Here we quantified gradients of air temperature, relative air humidity and vapour pressure deficits (VPD) along urban forest edge-to-interior transects with contrasting stand structures in six major cities across Europe. We performed continuous hourly microclimate measurements for two consecutive years and analysed the magnitude and depth of edge effects, as well as forest structural drivers of microclimatic variation.

Compared to rural temperate forests, we found that edge effects reached deeper into urban forests, at least up to 50 m. Throughout the year, urban forest edges were warmer and drier compared to forest interiors, with the largest differences occurring during summer and daytime. Not only maximum, but also mean and minimum temperatures were higher at the urban forest edge up to large edge distances (at least 85 m). Denser forests with a higher plant area index buffered high air temperatures and VPDs from spring to autumn.

We conclude that urban forest edges are unique ecotones with specific microclimates shaped by the UHI effect. Both forest edges and interiors showed increased buffering capacities with higher forest canopy density. We advocate for the conservation and expansion of urban forests which can buffer increasingly frequent and intense climate extremes. To this end, urban forest managers are encouraged to aim for multi-layered dense forest canopies and consider edge buffer zones of at least 50 m wide.

Keywords

Air temperature, edge effect, forest structure, microclimate, urban heat island, vapour pressure deficit

Introduction

Worldwide, an increasing proportion of humans are living in cities, towns and agglomerations (UN, 2019) which has led to a doubling of total land surface areas in cities between 1992 and 2015 (IPBES *et al.*, 2019). Urban areas possess unique ecological properties, with increased air and surface temperatures being some of its most important characteristics, a phenomenon called the 'urban heat island' (UHI) effect. UHIs are mainly caused by large amounts of imperviousness, heat storage in buildings and pavements and reduced evapotranspiration in the absence of vegetation (Oke, 2002; Kleerekoper *et al.*, 2012). The largest UHI intensities are typically recorded in summer (Arnfield, 2003; van Hove *et al.*, 2015), and specifically during the night due to the larger heat storage in urban areas and subsequent nightly release of heat from concrete, asphalt and building materials (Arnfield, 2003; Doick *et al.*, 2014; van Hove *et al.*, 2015). This timing of elevated temperatures has severe consequences for human health, well-being and mortality, given the association of hot nights with increased heat stress in humans (Roye *et al.*, 2021; He *et al.*, 2022).

Urban forests are generally defined as all forest and tree resources in (and close to) urban areas (Konijnendijk, 2003). Urban forests reduce hot temperatures and heatwaves in cities by lowering temperatures in the city area in the vicinity of the urban forest and by providing cool microclimate refugia beneath the canopy (Yan *et al.*, 2018; Ziter *et al.*, 2019; Wang *et al.*, 2021). Microclimates can be defined as fine-scale climate variations which are, at least temporarily, decoupled from the background atmosphere (macroclimate) (Bramer *et al.*, 2018). The microclimatic cooling in urban forests mainly happens through shading by the canopy and evaporative cooling induced by the transpiring trees, which consumes latent heat at the expense of sensible heat (Bramer *et al.*, 2018). Similarly, urban parks (with woody vegetation) have been shown to experience maximum summer temperatures up to 4 °C cooler compared to neighbouring streets and squares, thereby greatly reducing thermal stress (Cohen *et al.*, 2012; Doick *et al.*, 2014). The extent of microclimatic buffering by urban forests and parks is largely determined by structural characteristics, such as canopy cover, tree species identity and richness, but also topography (Feyisa *et al.*, 2014; Zellweger *et al.*, 2019; Schwaab *et al.*, 2021; Wang *et al.*, 2021). The buffering capacity of urban forests is crucial for the health of citizens living in urban areas (Smoyer *et al.*, 2000; Gillerot *et al.*, 2022; Iungman *et al.*, 2023), but can also substantially mitigate urban heat impacts on flora and fauna, such as temperatures that exceed species' thermal limits, as well as changes in phenology and pest infestations (Zipper *et al.*, 2016; Long *et al.*, 2019). For all these reasons, urban forests are increasingly proposed as a viable nature-based solution to moderate UHIs (van den Bosch & Ode Sang, 2017; Ziter *et al.*, 2019; Wang *et al.*, 2021; Iungman *et al.*, 2023).

Due to the strong fragmentation of urban landscapes (Moffatt *et al.*, 2004; Liu *et al.*, 2016; Olejniczak *et al.*, 2018), microclimatic buffering, however, can be reduced by edge effects (Horak, 2016; Li *et al.*, 2018). Steep microclimate gradients are generally found at forest edges with high incoming solar radiation and wind speeds (Matlack, 1993; Chen *et al.*, 1995; Meeussen *et al.*, 2021). Typically, mean and maximum air temperatures decrease from the forest edge into the interior, whereas minimum air temperatures and air humidity values tend to increase from edge to interior (Chen *et al.*, 1995; Saunders *et al.*, 1999; Schmidt *et al.*, 2017). The magnitude of these edge effects (Magnitude of Edge Influence; MEI) and how deep they extend into the forest (Depth of Edge Influence; DEI) are highly variable and determined by forest edge structure, edge orientation, local weather patterns and other factors (Matlack, 1993; Chen *et al.*, 1995). The DEI values reported in the scientific literature regarding microclimate variables, as temperature and air humidity, generally range between 5 and 30 m (Matlack, 1993; Gehlhausen *et al.*, 2000; Franklin *et al.*, 2021; Meeussen *et al.*, 2021), but can extend up to 200 m (Chen *et al.*, 1995). Consequently, given the unique environmental properties on the interface between urban forests and the city, urban forest edges may represent a novel, rapidly spreading ecotone (Hobbs *et al.*, 2014). However, studies at the forest-city interface are still largely lacking. This is an important knowledge gap because the UHI might exacerbate microclimatic edge effects, thereby reducing the buffering capacity of urban forests.

The few existing studies on urban forest edges indicate important changes in microclimate and temperature-related processes. Li *et al.* (2018) described edge microclimate patterns in an urban forest in Seoul, Republic of Korea, during the hottest three consecutive days in August 2016 and found significant edge effects for air temperature, relative humidity, soil temperature and soil moisture. Bae and Ryu (2021) also found changes in soil moisture and soil temperature at urban forest edges in Seoul, but only significantly for the west-oriented edge and not for the east-oriented edge due to the difference in adjacent land-use. Additionally, Garvey *et al.* (2022) showed increased soil temperature and reduced soil moisture in urban forest edges in Boston compared to rural forest edges in central Massachusetts, USA. Furthermore, in the Dane county, Wisconsin, USA, Latimer and Zuckerberg (2017) reported lower winter temperature minima in forest edges vs interiors, but higher winter minima when forests were closer to cities or had higher basal area values.

To better understand UHI effects on urban forest edges, we designed a study at the continental scale. We studied edge-to-interior gradients of urban forests in six cities across temperate Europe, which enabled us to generalise effects and consider regional context-dependencies. Additionally, we aimed to gain insights in the potential role of urban forest structure in mediating UHI effects. Therefore, two edge-to-interior gradients were set out in each urban forest, differing in forest structure (open vs. dense) given its important influence on forest microclimates (Zellweger *et al.*, 2019). To the best of our knowledge, there is no study yet that clarifies microclimatic changes along urban forest edge-to-interior gradients throughout the year at a continental scale. We performed continuous hourly microclimate measurements using microclimate sensors in the air (measuring temperature, relative air humidity and vapour pressure deficits) for two years to enable a comprehensive study of microclimate gradients in urban forest edges.

We hypothesize that:

1) The exposure to the UHI effect will result in **larger magnitude and depth of edge effects** on the microclimate in urban forest edges than known for rural forest edges.
2) The magnitude and depth of **edge effects by the UHI effect will be stronger when the forest structure is open compared to more dense.**
3) Not only daily maximum, but – in contrast to rural forest edges – **also daily minimum temperatures will be higher at urban forest edges** than interiors. We expect this effect on daily minimum temperatures to be largest during summer, as the UHI intensity is strongest in this season.
4) Finally, forest stands with higher density, basal area and shade-casting ability will show lower temperature maxima and VPD maxima in summer.

Materials & methods

Study regions and design

We studied six urban forests adjacent to large European cities (Figure 1), along a 1,400-km long macroclimatic gradient from Stockholm (Sweden) to Zurich (Switzerland). This results in significant climatological differences in temperature (monthly average minima of coldest month between -4.9 and 1°C, monthly average maxima of warmest month between 22.4 and 25°C) and mean annual precipitation (from 561 mm in Stockholm up to 1,107 mm in Zurich) (precipitation and temperatures are 30-year averages from Terraclimate 1981-2010, resolution of ~ 4 km (Abatzoglou *et al.*, 2018); Table S2). Urban-to-rural land surface temperature differences of summer daytime maxima range from +1.7 to +2.7 °C for the six studied European cities (CIESIN, 2016). We searched for large, deciduous forests bordering these cities, dominated by pedunculate oak (*Quercus robur*) to control for the effect of the dominant tree species between our selected urban forests. Pedunculate oak is one of the most dominant tree species of temperate deciduous forests in Europe (Barbati *et al.*, 2014), with high ecological and economic importance. Indeed, pedunculate oaks support a high number of associated species, rich woodland biodiversity (Eaton *et al.*, 2016; Mölder *et al.*, 2019) and provide high economical value (Mölder *et al.*, 2019; Şöhretoğlu & Renda, 2020). More environmental variables of the urban forests are given in Table S2.

In each of the six studied urban forests, we established twelve circular plots (9-m radius around a central tree) along a transect stretching from the urban forest edge (defined as the hypothetical line of tree stems at the edge closest to the urban area) into the core of the urban forest. These transects were 290 m to 3 km long and extended beyond the distance at which altered microclimatic conditions could be expected in rural forests (25-50 m, (Schmidt *et al.*, 2017))and even further given the larger spatial scale of UHI effects (e.g., > 50 m up to several km, Luo and Li (2014); Estoque et al. (2017); Ziter et al. (2019)). In each transect, plots were established in six pairs (Fig. S1). The first, second and third plot pair were located at approximately 5, 20 and 50 m from the forest edge (Fig. S2). The sixth pair was located in the forest interior at an average distance of 1600 m from the urban forest edge (range: 290-3260 m) while the fourth and fifth plot pair were located at intermediate distances (μ = 674 m, range = 85-1500 m for the fourth plot pair and μ = 994 m, range = 235-2090 m for the fifth plot pair) (Fig. S2). Within each plot pair, one plot had a denser forest canopy (i.e., high canopy cover; median tree and shrub cover being 88.5% and 37.5%, respectively; with multiple tree layers) and the other had a less dense forest canopy (i.e., more open canopy; median tree and shrub cover being 70% and 15%, respectively; with one tree layer). This contrast in stand structure allowed us to generate a difference in forest microclimate (Zellweger *et al.*, 2019; Meeussen *et al.*, 2021) within each of the six plot pairs. The distance between paired plots depended strongly on the region, but was on average 441 m (range: 21-1772 m).

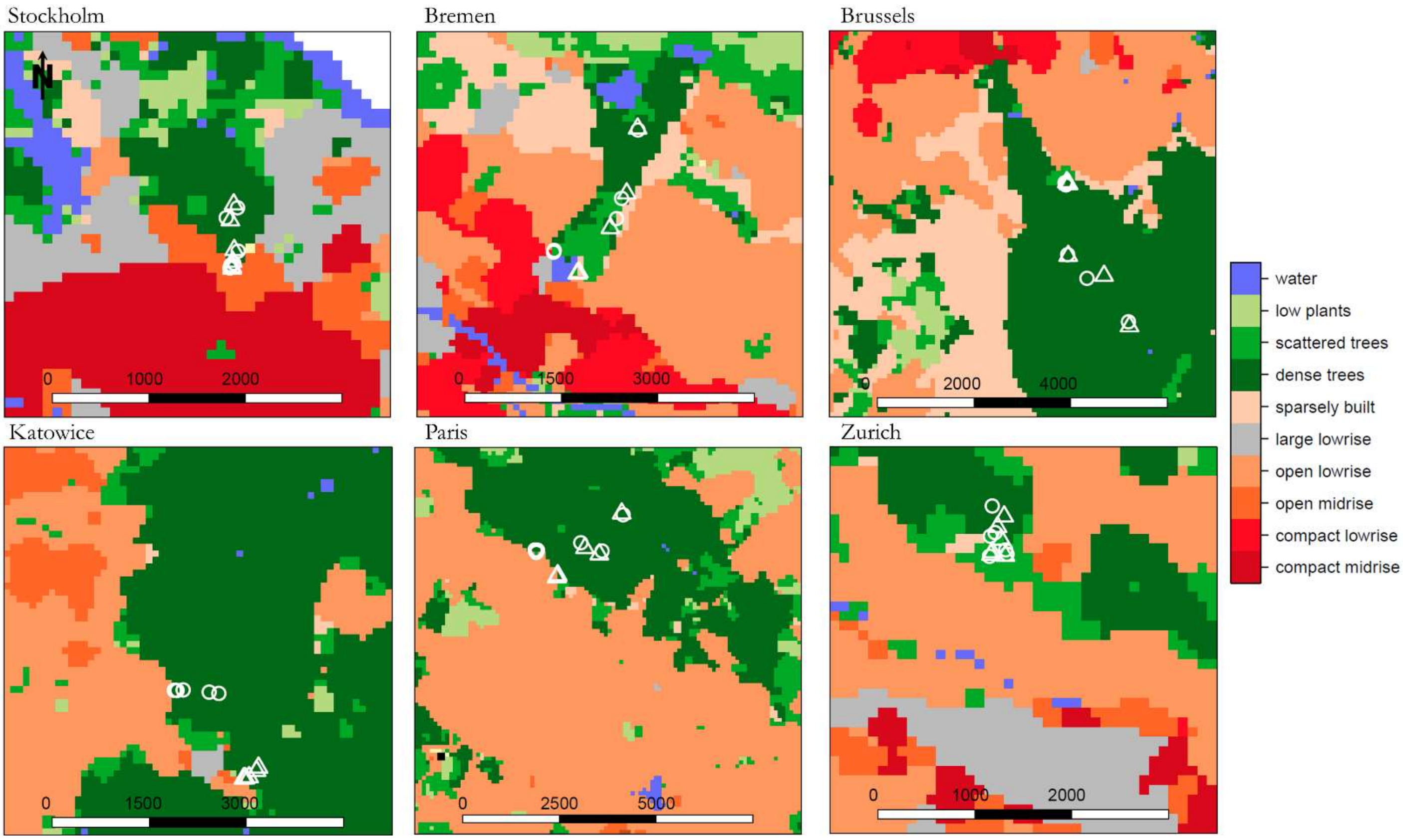

Figure 1. Land-use maps of urban forests and nearby cities. For each of the six urban forests, plots are shown as white circles for dense forest stands and triangles for open forest stands on a background map visualizing local climate zone categories. These categories map different types of built-up area and are standardly used in urban climatological studies (Stewart & Oke, 2012). Here, we used the European Local Climate Zone map produced by Demuzere *et al.* (2019) with a resolution of 100 m, a reported accuracy of 80% and is representative for the land-use in 2016. Scales were adjusted per panel to optimize plot visibility.

Microclimate measurements

Air temperature and relative humidity were measured with microclimate loggers (Lascar EL-USB-2, range of -35 to +80 °C and 0 to 100 %, accuracy of 0.45 °C and 3 %) attached to the north side of the central tree at a height of three meters to avoid vandalism or theft. The loggers were shielded from direct sunlight with a radiation shield as used in Zellweger *et al.* (2019). Measurements were performed hourly from September 2020 to August 2022. **Vapour pressure deficit** was calculated as the difference between the saturated (Psat) and actual water pressure in the air (Pair), which were derived from hourly temperature and relative humidity measurements following the formula of WMO (2008) (von Arx *et al.*, 2013) (eq. 1-3). Temperature, humidity and VPD values were then aggregated in daily mean, 5th and 95th percentile values (with 5th and 95th percentiles considered as daily minima and maxima excluding outliers).

$$Psat = 0.6112 \times \exp((17.62 \times T) / (T + 243.12)) \quad \textit{equation 1}$$

$$Pair = Psat \times RH/100 \qquad \textit{equation 2}$$

$$VPD = Psat - Pair \qquad \textit{equation 3}$$

In total, 8.4% of daily air temperature and 11.7% of daily air humidity values were missing due to empty batteries or erroneous measurements (Table S3). Gaps were filled with daily data from the closest plot with a similar forest structure. After gap filling, seasonal averages were calculated from daily mean, 5^{th} and 95^{th} percentile values. Seasons were considered as follows: autumn (01/09 – 30/11); winter (01/12 – 28/02); spring (01/03-31/05); and summer (01/06-31/08).

Environmental drivers

Apart from the distance to the urban forest edge, we also tested which forest structural and topographical characteristics could explain the variation in microclimate. To assess the forest structure in a plot, we determined the basal area of all trees and shrubs (diameter at breast height (DBH) > 7.5 cm) within the circular plot by two perpendicular DBH measurements with a calliper. These values were summed to calculate the basal area (BA; m^2 per ha) for each plot. For each species, the percentage canopy cover in tree layer (>7 m) and shrub layer (>1 m and <7 m) was visually estimated. Additionally, the percentage canopy cover was determined with a convex spherical densiometer (Baudry *et al.*, 2014) and calculated as the average of four densiometer readings in every plot, one in each cardinal direction at a distance of 4.5 m from the central tree. The shade-casting ability (SCA) of the overstorey was determined as the abundance-weighted mean of species-specific tree and shrub SCA scores ranging as ordinal numbers from 1 to 6 (1: low shade-casting ability e.g. *Betula pendula*, 6: very high shade-casting ability e.g. *Taxus baccata*; Table S1) weighted by the percentage canopy cover of each species in the tree and shrub layer of the plot (*sensu* Verheyen *et al.* (2012); De Lombaerde *et al.* (2019); Maes *et al.* (2019); Depauw *et al.* (2020)).

Finally, a highly detailed assessment of plant biomass from the ground surface to the canopy was performed with a RIEGL VZ-400 terrestrial laser scanner (RIEGL Laser Measurement Systems GmbH). The scanner was mounted on a tripod of approximately 1.45 m height and performed a scan in each plot with a zenith angle ranging from 30 to 130°. The data from this scan was registered with the RiSCAN PRO software (provided by RIEGL). From this data, the vertical distribution of plant area volume density (m^2/m^3) could be derived as profiles in function of canopy height. We integrated these profiles between 35 and 70° zenith angle to calculate a Plant Area Index (PAI), which is defined as the one-sided surface area of vegetation material per unit ground surface area. The PAI provides an accurate estimate of plant biomass including leaves and woody plant biomass and gives a good indication of the density of the stand structure (Calders *et al.*, 2015; Liang *et al.*, 2016; Meeussen *et al.*, 2020). The method is described in detail in Calders *et al.* (2014); Calders *et al.* (2018).

Topographic variables were derived from the European Copernicus digital elevation model (EU-DEMv1.1, resolution of 25 m) (EEA, 2017) and consisted of the elevation (m above sea level), slope (°) and northness index (ranging from +1 north to -1 south and calculated as the cosine of aspect given as 0 to 360 °N). Slope and aspect were derived with the *terrain* function from the package 'raster' (Hijmans, 2022).

Statistical analyses

All analyses were performed in R v.4.1.1 (R Development Core Team version 4.1.1, 2020) and data made available online (now already through a private figshare link: https://figshare.com/s/49840f2f1a1ed2c7798f). First, we assessed the magnitude and depth of edge effects on the different microclimatic response variables throughout the year (hypothesis 1). Then, we tested interaction effects between the distance to the forest edge and forest structure (hypothesis 2) and focused specifically on edge effects on daily minimum temperatures (hypothesis 3). Finally, we explored which forest structural variables were important in driving microclimatic variation and edge effects, while considering topographic variation (hypothesis 4).

1. Magnitude and depth of edge effects on the microclimate

We used linear mixed-effects models (LMMs) to infer the effect of the urban forest edge on the forest microclimate. The air temperature, air humidity and VPD were modelled as response variables with edge distance as a categorical predictor variable (P1 to P6) for which the interior plots (P6) were used as the reference category. We ran LMMs with the city ID as a random intercept term (6 city levels), to account for the hierarchical study design and spatial autocorrelation of plots within urban forests (Zuur *et al.*, 2009). Given that we included only one seasonally averaged value per plot in the models, we did not need to include additional random effect terms to control for temporal autocorrelation. Our LMMs were fitted with the function *lme* from the 'nlme' package (Pinheiro *et al.*, 2021): conditional and marginal R^2 were determined with the 'MuMIn' package (Barton, 2019). The marginal and conditional R^2 give the proportion of microclimate variance explained by the fixed and fixed plus random effects, respectively (Nakagawa & Schielzeth, 2013). For comparative purposes in terms of effect size, all predictors were standardised to unit variance and mean zero.

$$microclimate \sim edge\ distance + (1|city) \qquad \textit{equation 4}$$

2. Forest structure interaction with edge effects

To test whether the forest structure interacts with the depth of edge effects, we added a forest structure term to the equation and ran models with and without the interaction term between the forest structure and the edge distance (eq. 5 indicated with the interaction effect*). We ran a model selection with the dredge function from package MuMin (Barton, 2019). We looked at the best models based on the lowest corrected Akaike Information Criterion (AICc) value and checked whether the interaction term was retained in the single best model after model selection.

$$microclimate \sim edge\ distance\ + structure + \ edge\ distance\ * structure\ +\ (1|city) \qquad \textit{equation 5}$$

3. Magnitude of edge effects on daily temperature minima

Due to the UHI effect on minimum temperatures, we expected daily temperature minima to be higher at the urban forest edge. We tested this hypothesis with the same models as used to test magnitude and depth of edge effects for all microclimatic variables (see above statistical analyses 1. magnitude and depth of edge effects, eq.4).

4. Environmental drivers of microclimate in urban forest edges

To assess the importance of forest structural characteristics as drivers of microclimate, we modelled the microclimatic variables as a function of three different forest structural metrics (PAI, BA and SCA) while considering topographic features as important covariates (elevation, slope and northness). We used a similar approach as for the modelling of magnitude and depth of edge effects (see above, statistical analyses 1. magnitude and depth of edge effects) (eq. 6). All predictors were scaled to mean zero and unit variance before modelling, only elevation was scaled per city region given the much larger differences between city regions than within city regions. For all models, VIF values (variance inflation factors, *vif* function, package 'cars') were below 1.5 indicating no multicollinearity issues (Neter *et al.*, 1990).

$$microclimate \sim PAI + BA + SCA + elevation + slope + northness + (1|city) \qquad \textit{equation 6}$$

Results

Given the similarity of relative air humidity and VPD patterns, we limit the results and discussions here to VPD. Relative air humidity results can be found in the appendix (Fig. S3-S8).

1) Magnitude and depth of edge effects on the microclimate in urban forest edges (hypothesis 1).

We found significant edge effects on air temperature and vapour pressure deficits (VPD) (Fig. 2, Fig. 3). The magnitude of edge effects ranged from 0.17 to 1.16 °C for air temperature and 0.02 to 0.29 kPa for VPD. The largest values were generally found for daily maxima for air temperature and VPD (Fig. 2). There was considerable seasonal variation in the magnitude of the edge effects, with larger edge effects in summer and smaller edge effects in winter for both air temperature and VPD. Mean air temperatures and VPDs were 0.83°C [CI: 0.53-1.12] and 0.16 kPa [CI: 0.10-0.22] higher, respectively, at the forest edge (P1 plots) than in the forest interior in summer. Whereas in winter the differences amounted to 0.41°C [CI: 0.29-0.53] and 0.03 kPa [CI: 0.02-0.05], respectively. When looking at daily temperature and VPD maxima, these differences were even larger in summer, 1.16°C [CI: 0.44-1.88] and 0.29 kPa [CI: 0.16-0.42], and also in winter, 0.52°C [CI: 0.33-0.71] and 0.05 kPa [CI: 0.03-0.07].

We found deep edge effects for air temperature, up to at least 50 m for all microclimate variables. For mean and minimum air temperatures, edge effects even reached the fourth plot pairs, at an average distance of 674 m from the forest edge (range: 85-1500 m) (except for mean summer temperature). At these large distances, the magnitudes of the edge effects were small, but again quite consistent and significant throughout the year. For VPD, the depth of edge effects was constant in time, in contrast to the seasonal variation in the magnitude of edge effects (Fig. 2). The microclimate models to test depth and magnitude of edge effects had on average a marginal R^2 value of 0.15 (range: 0.004-0.27) and a conditional R^2 value of 0.70 (range: 0.35-0.99) (including models on relative air humidity, R^2 values and sample sizes are given for all models in Table S4).

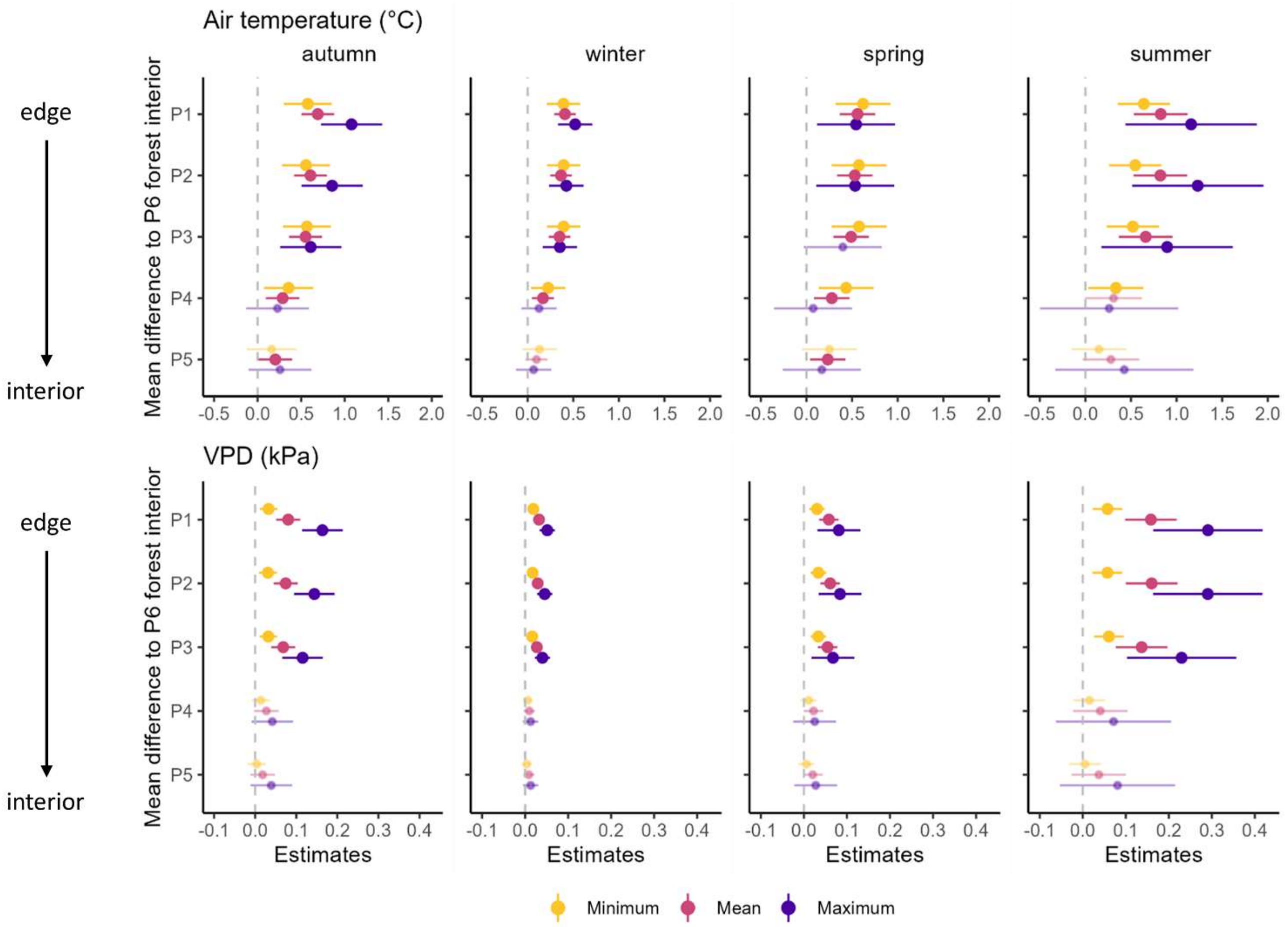

Figure 2 Estimates and 95% confidence intervals of the linear mixed-effects models we ran with the urban forest edge distance as the only fixed effect (equation 4). Nonsignificant variables (confidence interval overlapping zero) are made transparent using an alpha canal value of 0.4. The intercept term, or baseline for comparative purposes, was set to 'P6: forest interior plot' so that estimates are showing significant deviations (or not when crossing the vertical dotted line at zero) from the forest interior. Analyses were performed on seasonal averages of daily minimum, mean and maximum values.

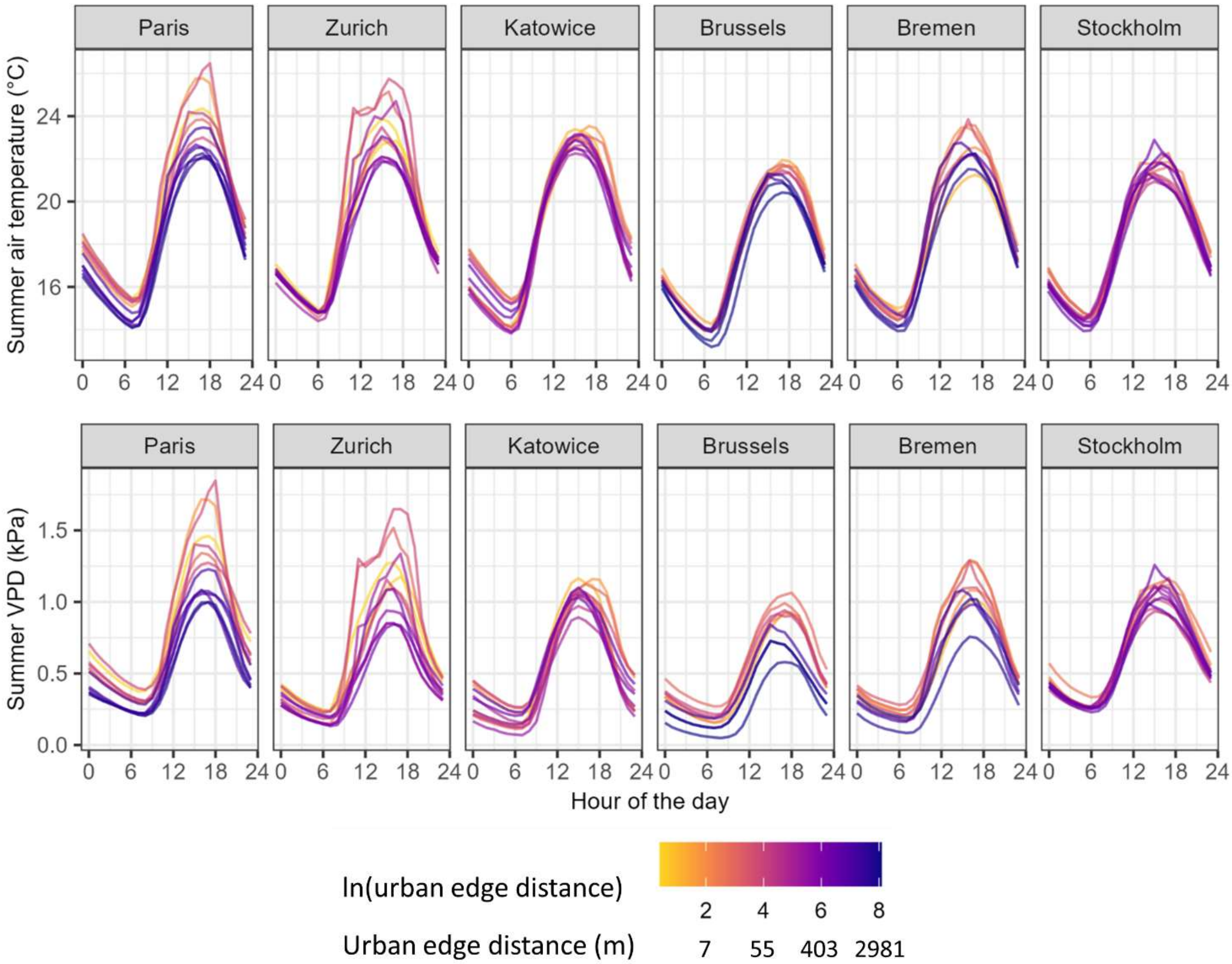

Figure 3 Daily cycles of summer microclimates in urban forest edges. The lines show summer averages of hourly microclimate measurements for each plot in this study's six urban forests (12 plots/city). The colour scale indicates the distance towards the urban forest edge given as a natural logarithm (ln(urban edge distance)).

2) Forest structure did not interact with edge effects, but can buffer the microclimate as an additive main effect (hypothesis 2).

We tested whether the forest structure interacted with the distance to the urban forest edge. For none of the 36 microclimate models (3 microclimate variables × daily min, mean and max statistics × 4 seasons, cf. equation 5), the interaction was retained in the best model after model selection with the dredge function (Table S5). This clearly indicated that the depth of edge effects did not change depending on the forest structure. Importantly, the forest structure was often included in the best model as main effect without the interaction, functioning as an additive effect next to the edge distance rather than an interactive effect. Irrespective of the distance to the forest edge, air temperatures and VPD were lowered in plots with a denser forest structure (Fig. 4). This effect and its diurnal and seasonal variation were analysed more in-depth below (4: environmental drivers of microclimate, as PAI, BA and SCA).

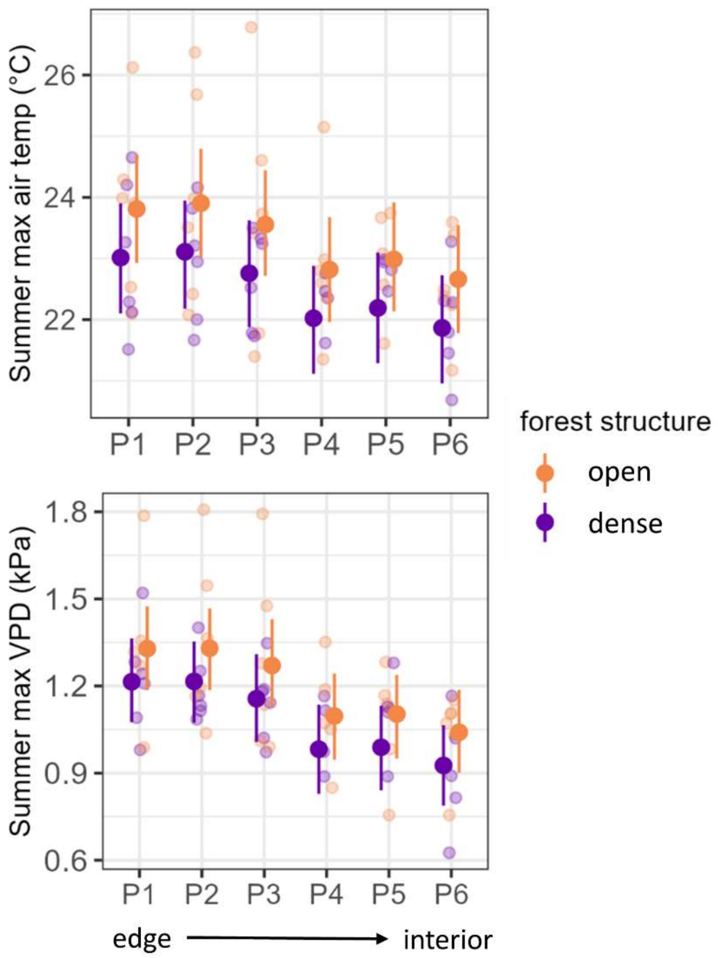

Figure 4 Summer microclimatic gradients from urban forest edge to interior. The smaller points show summer averages of daily microclimate measurements for plots (12 plots at each edge-to-interior location (6 regions * 2 structural types)). The larger points show model predictions, with 95% confidence intervals, based on the linear mixed-effects models with urban forest edge distance and forest structure as explanatory variables (equation 5).

Analyses were performed on seasonal averages of daily maximum values. Symbols were jittered on the x-axis for clarity.

3) Daily minimum temperatures were warmer at urban forest edges than interiors (hypothesis 3).

We found that daily air temperature minima were higher at urban forest edges compared with the forest interior (Fig. 2, Fig. 5). This edge effect was recorded throughout all four seasons of the year, being the weakest in winter (Fig. 5). During winter, urban forest edges (P1 plots) had approximately 0.39°C [CI: 0.21-0.58] warmer temperature minima compared to the forest interior. For autumn, spring and summer, the temperature minima in edges (P1 plots) were approximately 0.58°C [CI: 0.30-0.85], 0.62°C [CI: 0.32-0.92] and 0.64°C [CI: 0.35-0.93] warmer, respectively. The warmer temperatures reached deep into the urban forests up to the fourth plot pairs (P4 plots) (Fig. 2, Fig. 5), which were located at an average distance of 674m from the forest edge (range: 85-1500m). At these large distances to the edge, average temperature differences compared to the interior plot ranged from 0.22°C [CI: 0.04-0.41] in winter to 0.43°C [CI: 0.13-0.74] in spring.

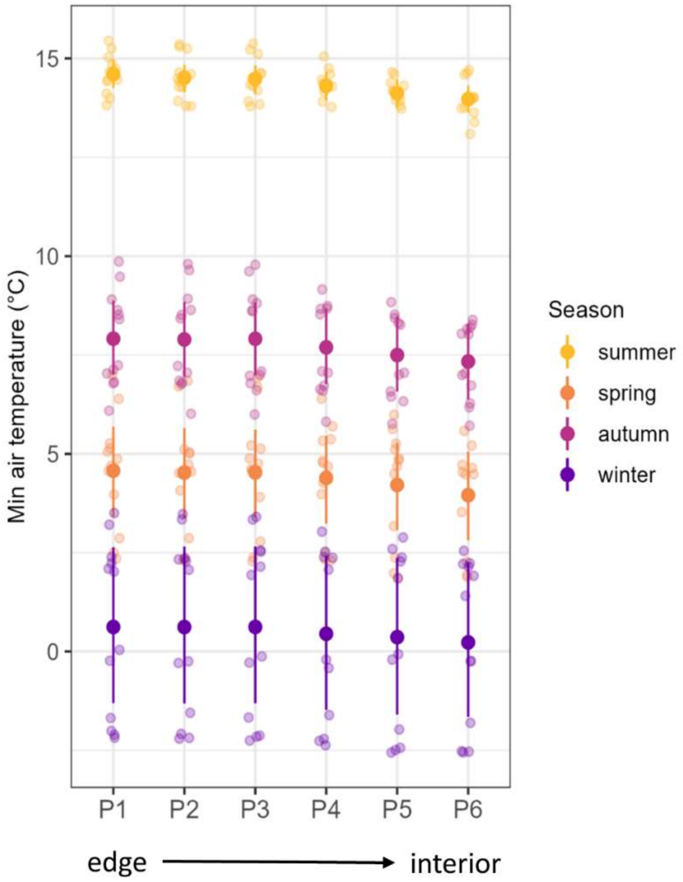

Figure 5 Seasonal minimum air temperature gradients from urban forest edge to interior. The smaller points show summer averages of daily microclimate measurements for plots (12 plots at each edge-to-interior location (6 regions * 2 structural types)). The larger points show model predictions, with 95% confidence intervals, based on the linear mixed models with urban forest edge distance as explanatory variable (equation 4). Analyses were performed on seasonal averages of daily minimum values. Symbols were jittered on the x-axis for clarity.

4) Environmental variables driving variation in microclimate (hypothesis 4).

Finally, we found that the forests' structure was an important determinant of the microclimate in urban forests and their edges. The Plant Area Index (PAI) was the most important structural driver of the microclimate in urban forests (Fig. 6). In urban forest stands with higher PAI values, the microclimate in the understorey consisted of lower maximum air temperatures throughout all seasons and lower mean air temperatures from spring to autumn (Fig. 6, Fig. S7, Fig. S9 for summer daily cycles). Furthermore, we found lower VPDs from spring to autumn for forest stands with higher PAI values (Fig. 6, Fig. S7, Fig. S9 for summer daily cycles). A classic forest structural metric, the basal area, did not significantly impact microclimate values and also the shade-casting ability (SCA) of the overstorey showed only a limited impact on the microclimate, a higher SCA led to warmer temperature minima in autumn and winter.

In addition to forest structure, we found a considerable influence of the topographic covariates. However, our study was not designed to assess topographic effects and most of the regions were generally flat, with Paris and Stockholm as exceptions. These topographic variables were therefore included in the models as covariates but we should be cautious in the interpretation as main effects. We found higher air temperatures and higher VPDs when the slope increased (Fig. 6). In Stockholm and Paris, the slope was highest at the urban forest edge and decreased towards the forest interior (significant edge effect on slope, see Fig. S10). The slope effect in the models indicating warmer and drier microclimates with increasing slope is thus probably caused by the correlated edge effect. Additionally, we found that summer and autumn air temperature maxima were lower at higher elevations (within the same urban forest), whereas air temperature minima were higher at higher elevations. Minimum VPD values increased slightly in autumn and spring with increasing elevation. Finally, also the aspect influenced the microclimate, forests on a more north-oriented slope had lower maximum VPDs in summer and autumn.

The microclimate models to test environmental drivers had on average a marginal R^2 value of 0.26 (range: 0.01-0.63) and conditional R^2 value of 0.65 (range: 0.16-0.99) (R^2 values and sample sizes are given for all models in Table S4).

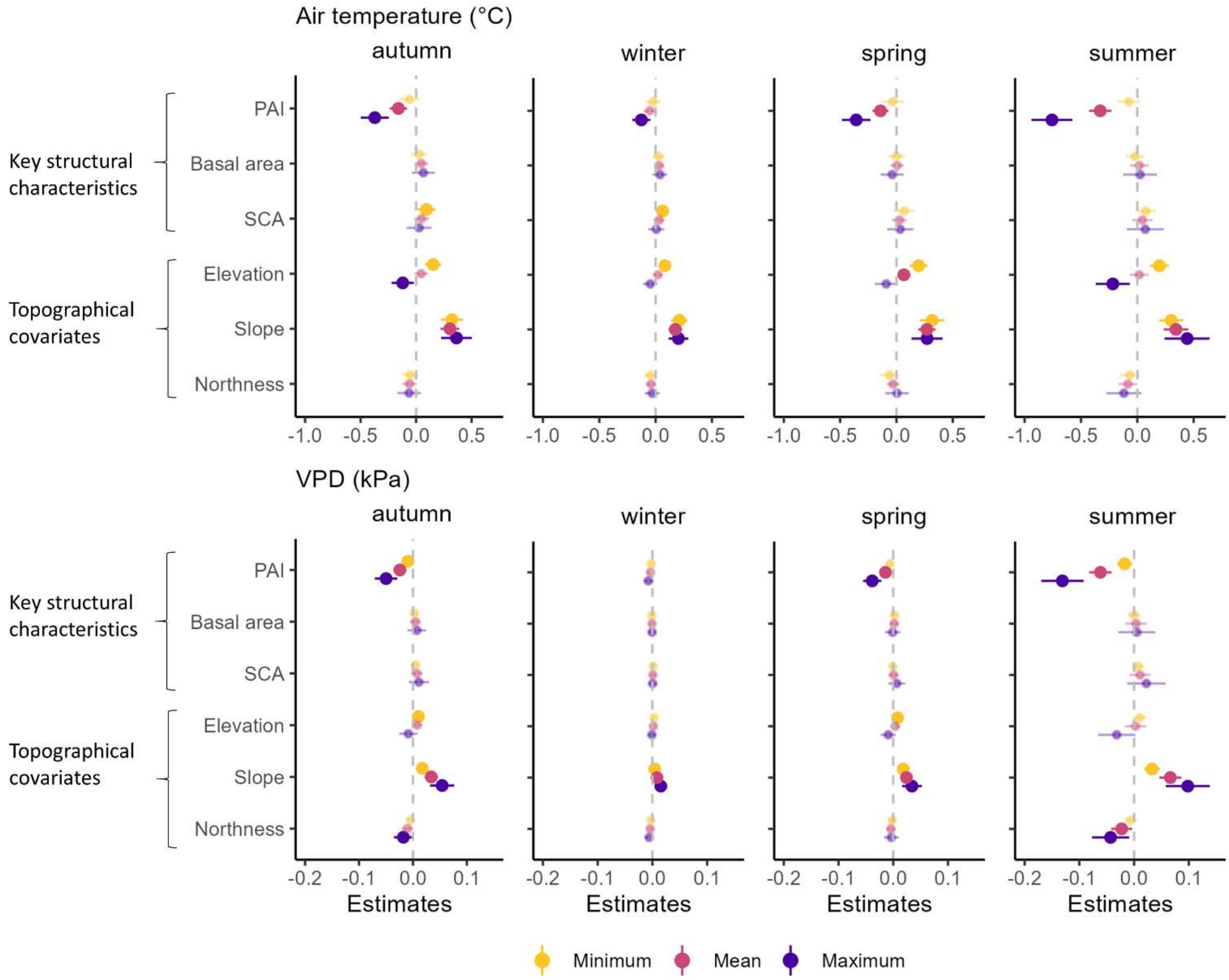

Figure 6 Estimates and 95% confidence intervals of the linear mixed-effects models we ran with environmental drivers as explanatory variables (equation 6). Nonsignificant variables (confidence interval overlapping zero) are made transparent. Analyses were performed on seasonal averages of daily minimum, mean and maximum values.

Discussion

1) Edge effects are of similar magnitude but reach deeper into urban forests, compared to rural forests (hypothesis 1)

The magnitudes of urban forest edge effects on temperature and vapour pressure deficit (VPD) were similar to values reported in previous microclimatic studies on edge effects in rural forests (Gehlhausen et al., 2000; Meeussen et al., 2021). Edge effects in urban forest edges are thus not necessarily larger in magnitude than in their rural counterparts. Nevertheless, these edge effects can have significant consequences for urban forests.

We found that urban forest edges were generally warmer and drier than urban forest interiors. Especially in summer, daily temperatures were on average 0.8 °C warmer and maximum temperatures were even 1.2 °C warmer in the urban forest edge compared to the urban forest interior. Such increases are significant since they already exceeded the 1°C climate warming compared to 1850–1900 baseline temperatures today (IPCC, 2018) and warming of around 1°C has been shown to affect plants growing in the understorey significantly. For example, open-top chambers that warmed understorey plants with ± 1°C compared to the surrounding forest understorey resulted in significant vegetation changes in terms of phenology, functional traits and community composition (De Frenne *et al.*, 2010; Smith *et al.*, 2012; Blondeel *et al.*, 2020; Govaert *et al.*, 2021). Previous research on UHI effects has focused on street trees and urban vs. rural forests (Frank & Backe, 2023). Both increases and decreases in the growth of urban trees have been reported, mainly depending on ambient temperature and water availability (Pretzsch *et al.*, 2017; Meineke & Frank, 2018; Sonti *et al.*, 2019). Our results suggest that growing conditions differ significantly between urban forest edges and interiors. Furthermore, we consider our results conservative as we measured the microclimate at 3 m height, microclimatic effects closer to the ground surface are probably more pronounced (De Frenne *et al.*, 2021). These microclimatic differences could affect growth rates and tree performance within urban forests, potentially leading to the formation of novel ecotones.

In terms of vapour pressure deficit, edges had on average 0.16 kPa higher VPDs than forest interiors (daily means) in summer and even 0.29 kPa higher VPD maxima. These conditions could make urban forest edges less suitable habitats for drought-sensitive species and drive community composition towards drought resistance. For example, terrestrial isopod communities change along forest edge-to-interior gradients and rural-to-urban gradients with more drought-resistant species in forest edges and urban areas (De Smedt et al., 2018; Ooms et al., 2020). Concerning plants and trees growing in urban forest edges, higher VPDs increase the evaporative demand, which makes it highly likely that they experience more pronounced drought stress. This in turn can hamper their growth and survival given that vapour pressure deficit has become a main factor constraining tree growth rates in central European forests (Trotsiuk et al., 2021). Furthermore, drought stress has been reported to be tightly linked to urban trees' vulnerability to insect pests and diseases (Dale & Frank, 2017; Meineke & Frank, 2018; McDowell *et al.*, 2020). Interactions between temperature and water stress, as well as insect pests, have been confirmed for the health and growth of street trees (Dale & Frank, 2014; Gillner *et al.*, 2014). Yet, research on these interactions in urban forests, focusing on forest trees and herbaceous plants, is still scarce (Frank & Backe, 2023). Finally, drier conditions at urban forest edges can alter soil ecosystem functions, for example, soil respiration (Vasenev *et al.*, 2021; Garvey *et al.*, 2022).

The edge effects reached up to 50 m into the urban forests for maximum air temperature, relative humidity and VPD, which is deeper than generally observed in rural contexts (10 to 30 m, as it is often reported, but in some cases up to 240 m) (Matlack, 1993; Chen *et al.*, 1995; Gehlhausen *et al.*, 2000; Schmidt *et al.*, 2017; Meeussen *et al.*, 2021). Mean and minimum air temperatures even differed significantly from interior temperatures for edge distances beyond 50 m (range: 85-1500 m, average: 674 m). From our measurements we conclude that edge effects in this study's six urban forests reach deeper then generally reported for rural forests. We encourage studies with a paired rural-urban forest edge design to confirm these differences in depth (but also the similar magnitude we found) of microclimatic edge effects between rural and urban forests. Given urban forests' fragmented nature, with high edge-to-interior ratios as a result, it is essential to consider these deep edge effects and their potential consequences for urban forest biodiversity, ecology and design.

2) A denser forest structure buffers the microclimate irrespective of edge distance (hypothesis 2 & 4).

We found that an increase in plant area index (PAI) could significantly reduce temperature maxima, increase relative air humidity and reduce vapour pressure deficits (VPD). The PAI is a representative metric for forest structural density (Liang *et al.*, 2016; Meeussen *et al.*, 2020) and shows to be stronger associated with microclimate buffering than basal area or shade-casting ability, confirming other recent studies (Zellweger *et al.*, 2019; Meeussen *et al.*, 2021). Forest managers can thus strongly impact the microclimate of urban forests by management actions. As such, dense and multi-layered canopies can be used to buffer the increasing summer temperatures and drought induced by UHIs and extended edge effects. Furthermore, we noted that PAI values were generally lower at the urban forest edge and tended to increase towards the forest interior (positive, but non-significant edge effect on

PAI, see Fig. S10), a pattern already described for rural edge-to-interior gradients and attributed to higher wind speeds and reduced canopy height at edges, openness of the façade of the edge, and to a different tree species composition including more species at the forest edge with a lower shade-tolerance, crown volume and branching density (Harper *et al.*, 2005; Delgado *et al.*, 2007; Meeussen *et al.*, 2020; Verhelst *et al.*, 2023). This edge-interior gradient in plant area index probably also contributed to the microclimatic edge effects we found (Hardwick *et al.*, 2015; Sanusi *et al.*, 2017; Meeussen *et al.*, 2021).

The relation between forest structure and microclimate buffering, however, can vary depending on regional climates and the local water cycle (Ehbrecht *et al.*, 2019). For example, von Arx *et al.* (2013) showed that during dry periods, the buffering capacities generally increased below dense canopies, yet decreased below sparse canopies. Also Davis *et al.* (2019) showed that especially forests with a sparse canopy cover, would lose buffering capacity in future water-limited regions. Furthermore, recent research showed that in stands with lower basal area, the transpiration sensitivity of trees to high VPD values increased (Bachofen *et al.*, 2023). Additionally, regional differences in cloud cover and its seasonality can affect surface temperatures and the strength of urban heat islands (Dai *et al.*, 1999; Morris *et al.*, 2001). Furthermore, the size, shape and position within the city might affect urban forest microclimates as well (Jaganmohan *et al.*, 2016; Sodoudi *et al.*, 2018; Zhu *et al.*, 2022). These regional differences were controlled for in this study, but not explicitly investigated due to the limited number of urban forests (n=6). However, we advocate for future studies including a large number of urban forests of varying sizes and shapes across different climate types to explore these topics.

Topography was included as a covariate in the statistical analyses because of the range in elevation, especially pronounced in Stockholm and Paris. In those two regions, the slope was highest at the urban forest edge and decreased towards the forest interior (significant edge effect on slope, see Fig. S10). The slope effect in these models indicating warmer and drier microclimates with increasing slope is thus probably caused by the correlated edge effect. We also reported some small effects of elevation and we found lower summer temperatures and VPDs for more north-oriented forest plots (Bennie *et al.*, 2008). These effects were small and should be interpreted with caution given the limited variability of elevation, slope and aspect in our dataset.

3) Daily minimum temperatures were warmer at urban forest edges than interiors throughout all seasons (hypothesis 3).

Contrary to the common microclimatic theory and findings stating that forest edges show more extreme warm and cold temperatures than forest interiors, we found minimum temperatures to be warmer at the forest edges than in forest interiors throughout the whole year. These findings support our hypothesis that the UHI effect can change edge-to-interior microclimate patterns, especially in terms of minimum temperatures. Urban forest edges experience less cooling during the night than the forest interior. In summer, species at the urban forest edge might be exposed to more heat stress because they experience a shorter time period for recovery at night. During winter, cold extremes are less intense at the urban forest edge, which could enhance the survival of warm-adapted species and exotic species which often originate from warmer regions (Géron *et al.*, 2021). For example, Brice *et al.* (2014) found a higher abundance of cold-intolerant lianas in temperate forests in more urbanized landscapes and forest edges. Additionally, vegetation at the urban forest edge might be less exposed to spring frost and experience a longer growing season than the forest interior.

In their recent review, Frank and Backe (2023) teased apart the local and landscape effects of UHIs on forests. They mention that temperatures will be consistently warmer, in general and specifically during the night, within forests that are surrounded by urbanized landscapes. The significantly higher daily mean and minimum temperatures we found at exceptionally large distances from the urban forest edge could be interpreted as a landscape-scale UHI effect and less so as a local edge effect extending very deep into the urban forest. This observation is supported by the typically strong edge effects we found on daily maximum temperatures, which we reported only up to the shorter distance of 50 m away from the edge. Therefore, we argue that we observed both local-scale UHI effects as deep edge effects (up to 50 m) and landscape-scale effects as general warming of the forests up to a considerable distance, especially at night.

4) Implications for urban forest management

Preserving structurally dense and at least 50 m wide edge buffer zones and existing urban forests that provide forest interior habitat will ensure the presence of maximally buffered forest interior as a refuge for urban biodiversity and citizens during summer heat waves. Furthermore, our results suggest that forest managers can increase the buffering capacity of urban forests by managing for dense or multi-layered canopies. These measures can greatly reduce maximum daytime summer temperatures and thus help to mitigate the negative impact of the UHI effect on human well-being and on the biodiversity in the forest. However, the cooling of night-time temperatures cannot be achieved by management interventions in the forest. To reach lower night-time temperatures, a reduction of the UHI itself is needed by other measures, such as increasing the tree cover within the city or using cool green roofs or pavements (Li *et al.*, 2014; Wang & Akbari, 2016; Ziter *et al.*, 2019; Winbourne *et al.*, 2020). Finally, the choice of tree species in urban forests is becoming increasingly important in the context of UHIs. For example, the UHI could lead to (drought) stress and consequent changes in the emission of biogenic volatile organic compounds (BVOC) in trees (Niinemets, 2010; Calfapietra *et al.*, 2015; Seco *et al.*, 2015). Considering species' VOC emission potential thus becomes increasingly important for urban forest managers to avoid a negative effect of trees on the city's air quality (Calfapietra *et al.*, 2013; Curtis *et al.*, 2014). Additionally, the UHI could amplify climate change effects (Esperon-Rodriguez *et al.*, 2020; Hirons *et al.*, 2021). A recent study calculated that more than half of tree and shrub species planted in cities are growing in climatic conditions that exceed the temperature range observed across their biogeographic distribution and even 65% of tree and shrub species in terms of precipitation ranges. These numbers are expected to rise further with continuing climate change and clearly demonstrate how crucial the choice of species becomes for the future of urban forests (Esperon-Rodriguez *et al.*, 2022).

Conclusion and outlook

Urban forest edges were warmer and drier throughout the whole year, than the urban forest interior and these microclimatic changes reached up to 50 m into urban forests. In addition, we found that daily mean and minimum temperatures were raised by the UHI effect, not only at the urban forest edge but also at large distances within forest interiors. Potential consequences for forest health, productivity and biodiversity at urban forest edges can be expected but have yet to be investigated. We conclude that urban forest edges represent unique forest-city-ecotones characterised by specific microclimates. Urban forest edge-to-interior gradients could thus help us understand the future risks for both urban and rural forests in terms of climate extremes. To conserve and expand the capacity of urban forests to buffer the negative impacts of climate extremes, we encourage urban forest managers to aim for multi-layered dense forest canopies and consider edge buffer zones of at least 50 m.

Acknowledgements

The authors thank Luc Willems, Robbe De Beelde, Kris Ceunen for technical support with the fieldwork and laboratory analyses. The authors thank Thomas Vanneste, Eliza Steffen, Lorenzo Ferrini and Michał Lipa for help with the fieldwork, Patrick Huvenne, Frederik Vaes (Belgium), Matthieu Bourre and Séverine Rouet (France) and Grzegorz Skurczak (Sweden, Djurgårdsförvaltningen) for permission to conduct the research in the urban forests, and Tomasz Krupa for help in selecting the suitable study sites in Katowice.

Funding

This work was supported by the Research Foundation Flanders (FWO) (K.D.P. ASP035-19, LD 1221523N), the European Research Council (ERC) (ERC Starting Grant FORMICA 757833, 2018, http://www.formica.ugent.be) and the FWO Scientific research network FLEUR (http://www.fleur.ugent.be). JL acknowledges funding from the Agence Nationale de la Recherche (ANR) (project IMPRINT; grant nr. ANR-19-CE32-0005-01). FZ was supported by the Swiss National Science Foundation (grant nr. 193645). SAOC was funded by Bolin Centre for Climate Research.

Competing interests

The authors have no relevant financial or non-financial interests to disclose.

Author contributions

KDP, PDF, PV, LD and KV conceived the ideas and designed methodology; all authors collected data; KDP led the data analyses and the writing of the manuscript. All authors contributed critically to the drafts and gave final approval for publication.

Data availability statement

Data will be made available online (through Figshare) and is now already accessible through a private link: https://figshare.com/s/49840f2f1a1ed2c7798f.

Bibliography

Abatzoglou JT, Dobrowski SZ, Parks SA, Hegewisch KC. 2018. TerraClimate, a high-resolution global dataset of monthly climate and climatic water balance from 1958–2015. *Scientific Data* **5**(1): 170191.

Arnfield AJ. 2003. Two decades of urban climate research: a review of turbulence, exchanges of energy and water, and the urban heat island. *International Journal of Climatology* **23**(1): 1-26.

Bachofen C, Poyatos R, Flo V, Martínez-Vilalta J, Mencuccini M, Granda V, Grossiord C. 2023. Stand structure of Central European forests matters more than climate for transpiration sensitivity to VPD. *Journal of Applied Ecology* **60**(5): 886-897.

Bae J, Ryu Y. 2021. The magnitude and causes of edge effects on soil organic carbon stocks within and across urban to rural forest patches. *Landscape and Urban Planning* **215**: 104223.

Barbati A, Marchetti M, Chirici G, Corona P. 2014. European Forest Types and Forest Europe SFM indicators: Tools for monitoring progress on forest biodiversity conservation. *Forest Ecology and Management* **321**: 145-157.

Barton K. 2019. MuMIn: Multi-Model Inference.

Baudry O, Charmetant C, Collet C, Ponette Q. 2014. Estimating light climate in forest with the convex densiometer: operator effect, geometry and relation to diffuse light. *European Journal of Forest Research* **133**(1): 101-110.

Bennie J, Huntley B, Wiltshire A, Hill MO, Baxter R. 2008. Slope, aspect and climate: Spatially explicit and implicit models of topographic microclimate in chalk grassland. *Ecological Modelling* **216**(1): 47-59.

Blondeel H, Perring MP, De Lombaerde E, Depauw L, Landuyt D, Govaert S, Maes SL, Vangansbeke P, De Frenne P, Verheyen K. 2020. Individualistic responses of forest herb traits to environmental change. *Plant Biology* **22**(4): 601-614.

Bramer I, Anderson BJ, Bennie J, Bladon AJ, De Frenne P, Hemming D, Hill RA, Kearney MR, Korner C, Korstjens AH, et al. 2018. Advances in Monitoring and Modelling Climate at Ecologically Relevant Scales. In: Bohan DA, Dumbrell AJ, Woodward G, Jackson M eds. *Next Generation Biomonitoring, Pt 1*. San Diego: Elsevier Academic Press Inc, 101-161.

Brice M-H, Bergeron A, Pellerin S. 2014. Liana distribution in response to urbanization in temperate forests. *Écoscience* **21**(2): 104-113.

Calders K, Armston J, Newnham G, Herold M, Goodwin N. 2014. Implications of sensor configuration and topography on vertical plant profiles derived from terrestrial LiDAR. *Agricultural and Forest Meteorology* **194**: 104-117.

Calders K, Newnham G, Burt A, Murphy S, Raumonen P, Herold M, Culvenor D, Avitabile V, Disney M, Armston J, et al. 2015. Nondestructive estimates of above-ground biomass using terrestrial laser scanning. *Methods in Ecology and Evolution* **6**(2): 198-208.

Calders K, Origo N, Disney M, Nightingale J, Woodgate W, Armston J, Lewis P. 2018. Variability and bias in active and passive ground-based measurements of effective plant, wood and leaf area index. *Agricultural and Forest Meteorology* **252**: 231-240.

Calfapietra C, Fares S, Manes F, Morani A, Sgrigna G, Loreto F. 2013. Role of Biogenic Volatile Organic Compounds (BVOC) emitted by urban trees on ozone concentration in cities: A review. *Environmental Pollution* **183**: 71-80.

Calfapietra C, Peñuelas J, Niinemets Ü. 2015. Urban plant physiology: adaptation-mitigation strategies under permanent stress. *Trends in Plant Science* **20**(2): 72-75.

Chen J, Franklin JF, Spies TA. 1995. Growing-Season Microclimatic Gradients from Clearcut Edges into Old-Growth Douglas-Fir Forests. *Ecological Applications* **5**(1): 74-86.

CIESIN 2016. Global Urban Heat Island (UHI) Data Set, 2013.In Center for International Earth Science Information Network (CIESIN) CU. Palisades, New York: NASA Socioeconomic Data and Applications Center (SEDAC).

Cohen P, Potchter O, Matzarakis A. 2012. Daily and seasonal climatic conditions of green urban open spaces in the Mediterranean climate and their impact on human comfort. *Building and Environment* **51**: 285-295.

Curtis AJ, Helmig D, Baroch C, Daly R, Davis S. 2014. Biogenic volatile organic compound emissions from nine tree species used in an urban tree-planting program. *Atmospheric Environment* **95**: 634-643.

Dai A, Trenberth KE, Karl TR. 1999. Effects of Clouds, Soil Moisture, Precipitation, and Water Vapor on Diurnal Temperature Range. *Journal of Climate* **12**(8): 2451-2473.

Dale AG, Frank SD. 2014. The Effects of Urban Warming on Herbivore Abundance and Street Tree Condition. *Plos One* **9**(7): e102996.

Dale AG, Frank SD. 2017. Warming and drought combine to increase pest insect fitness on urban trees. *Plos One* **12**(3): e0173844.

Davis KT, Dobrowski SZ, Holden ZA, Higuera PE, Abatzoglou JT. 2019. Microclimatic buffering in forests of the future: the role of local water balance. *Ecography* **42**(1): 1-11.

De Frenne P, De Schrijver A, Graae BJ, Gruwez R, Tack W, Vandelook F, Hermy M, Verheyen K. 2010. The use of open-top chambers in forests for evaluating warming effects on herbaceous understorey plants. *Ecological Research* **25**(1): 163-171.

De Frenne P, Lenoir J, Luoto M, Scheffers BR, Zellweger F, Aalto J, Ashcroft MB, Christiansen DM, Decocq G, De Pauw K, et al. 2021. Forest microclimates and climate change: Importance, drivers and future research agenda. *Global Change Biology*(27): 2279-2297.

De Lombaerde E, Verheyen K, Van Calster H, Baeten L. 2019. Tree regeneration responds more to shade casting by the overstorey and competition in the understorey than to abundance per se. *Forest Ecology and Management* **450**: 12.

Delgado JD, Arroyo NL, Arévalo JR, Fernández-Palacios JM. 2007. Edge effects of roads on temperature, light, canopy cover, and canopy height in laurel and pine forests (Tenerife, Canary Islands). *Landscape and Urban Planning* **81**(4): 328-340.

Demuzere M, Bechtel B, Middel A, Mills G. 2019. Mapping Europe into local climate zones. *Plos One* **14**(4): e0214474.

Depauw L, Perring MP, Landuyt D, Maes SL, Blondeel H, De Lombaerde E, Brumelis G, Brunet J, Closset-Kopp D, Czerepko J, et al. 2020. Light availability and land-use history drive biodiversity and functional changes in forest herb layer communities. *Journal of Ecology* **108**(4): 1411-1425.

Doick KJ, Peace A, Hutchings TR. 2014. The role of one large greenspace in mitigating London's nocturnal urban heat island. *Science of the Total Environment* **493**: 662-671.

Eaton E, Caudullo G, Oliveira S, de Rigo D 2016. Quercus robur and Quercus petraea in Europe: distribution, habitat, usage and threats. In: San-Miguel-Ayanz J, de Rigo D, Caudullo G, Houston Durrant T, Mauri A eds. *European Atlas of Forest Tree Species*. Luxembourg: Publication Office of the European Union, 160-163.

EEA EEA 2017. EU-DEM v1.1.In European Environment A: Land Monitoring Service.

Ehbrecht M, Schall P, Ammer C, Fischer M, Seidel D. 2019. Effects of structural heterogeneity on the diurnal temperature range in temperate forest ecosystems. *Forest Ecology and Management* **432**: 860-867.

Esperon-Rodriguez M, Rymer PD, Power SA, Challis A, Marchin RM, Tjoelker MG. 2020. Functional adaptations and trait plasticity of urban trees along a climatic gradient. *Urban Forestry & Urban Greening* **54**: 126771.

Esperon-Rodriguez M, Tjoelker MG, Lenoir J, Baumgartner JB, Beaumont LJ, Nipperess DA, Power SA, Richard B, Rymer PD, Gallagher RV. 2022. Climate change increases global risk to urban forests. *Nature Climate Change*.

Estoque RC, Murayama Y, Myint SW. 2017. Effects of landscape composition and pattern on land surface temperature: An urban heat island study in the megacities of Southeast Asia. *The Science of the total environment* **577**: 349-359.

Feyisa GL, Dons K, Meilby H. 2014. Efficiency of parks in mitigating urban heat island effect: An example from Addis Ababa. *Landscape and Urban Planning* **123**: 87-95.

Frank SD, Backe KM. 2023. Effects of Urban Heat Islands on Temperate Forest Trees and Arthropods. *Current Forestry Reports* **9**(1): 48-57.

Franklin CMA, Filicetti AT, Nielsen SE. 2021. Seismic line width and orientation influence microclimatic forest edge gradients and tree regeneration. *Forest Ecology and Management* **492**: 13.

Garvey SM, Templer PH, Pierce EA, Reinmann AB, Hutyra LR. 2022. Diverging patterns at the forest edge: Soil respiration dynamics of fragmented forests in urban and rural areas. *Global Change Biology* **28**: 3094-3109.

Gehlhausen SM, Schwartz MW, Augspurger CK. 2000. Vegetation and microclimatic edge effects in two mixed-mesophytic forest fragments. *Plant Ecology* **147**(1): 21-35.

Géron C, Lembrechts JJ, Borgelt J, Lenoir J, Hamdi R, Mahy G, Nijs I, Monty A. 2021. Urban alien plants in temperate oceanic regions of Europe originate from warmer native ranges. *Biological Invasions*.

Gillerot L, Landuyt D, Oh R, Chow W, Haluza D, Ponette Q, Jactel H, Bruelheide H, Jaroszewicz B, Scherer-Lorenzen M, et al. 2022. Forest structure and composition alleviate human thermal stress. *Global Change Biology*.

Gillner S, Bräuning A, Roloff A. 2014. Dendrochronological analysis of urban trees: climatic response and impact of drought on frequently used tree species. *Trees* **28**: 1079 - 1093.

Govaert S, Vangansbeke P, Blondeel H, Steppe K, Verheyen K, De Frenne P. 2021. Rapid thermophilization of understorey plant communities in a 9 year-long temperate forest experiment. *Journal of Ecology* **109**(6): 2434-2447.

Hardwick SR, Toumi R, Pfeifer M, Turner EC, Nilus R, Ewers RM. 2015. The relationship between leaf area index and microclimate in tropical forest and oil palm plantation: Forest disturbance drives changes in microclimate. *Agricultural and Forest Meteorology* **201**: 187-195.
Harper KA, MacDonald SE, Burton PJ, Chen J, Brosofske KD, Saunders SC, Euskirchen ES, Roberts D, Jaiteh MS, Esseen P-A. 2005. Edge Influence on Forest Structure and Composition in Fragmented Landscapes. *Conservation Biology* **19**(3): 768-782.
He C, Kim H, Hashizume M, Lee W, Honda Y, Kim SE, Kinney PL, Schneider A, Zhang YQ, Zhu YX, et al. 2022. The effects of night-time warming on mortality burden under future climate change scenarios: a modelling study. *Lancet Planetary Health* **6**(8): E648-E657.
Hijmans R 2022. raster: Geographic Data Analysis and Modeling. R package version 3.6-11.
Hirons AD, Watkins JHR, Baxter TJ, Miesbauer JW, Male-Muñoz A, Martin KWE, Bassuk NL, Sjöman H. 2021. Using botanic gardens and arboreta to help identify urban trees for the future. *PLANTS, PEOPLE, PLANET* **3**(2): 182-193.
Hobbs RJ, Higgs E, Hall CM, Bridgewater P, Chapin III FS, Ellis EC, Ewel JJ, Hallett LM, Harris J, Hulvey KB, et al. 2014. Managing the whole landscape: historical, hybrid, and novel ecosystems. *Frontiers in Ecology and the Environment* **12**(10): 557-564.
Horak J. 2016. Suitability of biodiversity-area and biodiversity-perimeter relationships in ecology: a case study of urban ecosystems. *Urban Ecosystems* **19**(1): 131-142.
IPBES, Diaz S, Settele J, Brondizio ES, Ngo HT, Guèze M, Agard J, Arneth A, Balvanera P, Brauman KA, et al. 2019. Summary for policymakers of the global assessment report on biodiversity and ecosystem services of the Intergovernmental Science-Policy Platform on Biodiversity and Ecosystem Services. Bonn, Germany: IPBES secretariat.
IPCC. 2018. Global Warming of 1.5°C. An IPCC Special Report on the impacts of global warming of 1.5°C above pre-industrial levels and related global greenhouse gas emission pathways, in the context of strengthening the global response to the threat of climate change, sustainable development, and efforts to eradicate poverty. Geneva, Switzerland: World Meteorological Organization.
Iungman T, Cirach M, Marando F, Pereira Barboza E, Khomenko S, Masselot P, Quijal-Zamorano M, Mueller N, Gasparrini A, Urquiza J, et al. 2023. Cooling cities through urban green infrastructure: a health impact assessment of European cities. *The Lancet*.
Jaganmohan M, Knapp S, Buchmann CM, Schwarz N. 2016. The Bigger, the Better? The Influence of Urban Green Space Design on Cooling Effects for Residential Areas. *Journal of Environmental Quality* **45**(1): 134-145.
Kleerekoper L, van Esch M, Salcedo TB. 2012. How to make a city climate-proof, addressing the urban heat island effect. *Resources, Conservation and Recycling* **64**: 30-38.
Konijnendijk CC. 2003. A decade of urban forestry in Europe. *Forest Policy and Economics* **5**(2): 173-186.
Latimer CE, Zuckerberg B. 2017. Forest fragmentation alters winter microclimates and microrefugia in human-modified landscapes. *Ecography* **40**(1): 158-170.
Li D, Bou-Zeid E, Oppenheimer M. 2014. The effectiveness of cool and green roofs as urban heat island mitigation strategies. *Environmental Research Letters* **9**(5): 055002.
Li Y, Kang W, Han Y, Song Y. 2018. Spatial and temporal patterns of microclimates at an urban forest edge and their management implications. *Environmental Monitoring and Assessment* **190**(2).
Liang XL, Kankare V, Hyyppa J, Wang YS, Kukko A, Haggren H, Yu XW, Kaartinen H, Jaakkola A, Guan FY, et al. 2016. Terrestrial laser scanning in forest inventories. *Isprs Journal of Photogrammetry and Remote Sensing* **115**: 63-77.
Liu Z, He C, Wu J. 2016. The Relationship between Habitat Loss and Fragmentation during Urbanization: An Empirical Evaluation from 16 World Cities. *Plos One* **11**(4): e0154613.
Long LC, D'Amico V, Frank SD. 2019. Urban forest fragments buffer trees from warming and pests. *Science of the Total Environment* **658**: 1523-1530.
Luo X, Li W. 2014. Scale effect analysis of the relationships between urban heat island and impact factors: case study in Chongqing. *Journal of Applied Remote Sensing* **8**(1): 084995.
Maes SL, Blondeel H, Perring MP, Depauw L, Brūmelis G, Brunet J, Decocq G, den Ouden J, Härdtle W, Hédl R, et al. 2019. Litter quality, land-use history, and nitrogen deposition effects on topsoil conditions across European temperate deciduous forests. *Forest Ecology and Management* **433**: 405-418.
Matlack GR. 1993. Microenvironment variation within and among forest edge sites in the eastern United-States. *Biological Conservation* **66**(3): 185-194.

McDowell NG, Allen CD, Anderson-Teixeira K, Aukema BH, Bond-Lamberty B, Chini L, Clark JS, Dietze M, Grossiord C, Hanbury-Brown A, et al. 2020. Pervasive shifts in forest dynamics in a changing world. *Science* **368**(6494): eaaz9463.

Meeussen C, Govaert S, Vanneste T, Bollmann K, Brunet J, Calders K, Cousins SAO, De Pauw K, Diekmann M, Gasperini C, et al. 2021. Microclimatic edge-to-interior gradients of European deciduous forests. *Agricultural and Forest Meteorology* **311**: 108699.

Meeussen C, Govaert S, Vanneste T, Calders K, Bollmann K, Brunet J, Cousins SAO, Diekmann M, Graae BJ, Hedwall PO, et al. 2020. Structural variation of forest edges across Europe. *Forest Ecology and Management* **462**.

Meineke EK, Frank SD. 2018. Water availability drives urban tree growth responses to herbivory and warming. *Journal of Applied Ecology* **55**(4): 1701-1713.

Moffatt SF, McLachlan SM, Kenkel NC. 2004. Impacts of land use on riparian forest along an urban – rural gradient in southern Manitoba. *Plant Ecology* **174**(1): 119-135.

Mölder A, Meyer P, Nagel R-V. 2019. Integrative management to sustain biodiversity and ecological continuity in Central European temperate oak (Quercus robur, Q. petraea) forests: An overview. *Forest Ecology and Management* **437**: 324-339.

Morris CJG, Simmonds I, Plummer N. 2001. Quantification of the Influences of Wind and Cloud on the Nocturnal Urban Heat Island of a Large City. *Journal of Applied Meteorology* **40**(2): 169-182.

Nakagawa S, Schielzeth H. 2013. A general and simple method for obtaining R2 from generalized linear mixed-effects models. *Methods in Ecology and Evolution* **4**(2): 133-142.

Neter J, Wasserman W, Kutner MH. 1990. *Applied linear statistical models. Regression, analysis of variance, and experimental design.* Homewood, USA: Irwin.

Niinemets Ü. 2010. Mild versus severe stress and BVOCs: thresholds, priming and consequences. *Trends in Plant Science* **15**(3): 145-153.

Oke TR. 2002. *Boundary layer climates*: Routledge.

Olejniczak MJ, Spiering DJ, Potts DL, Warren RJ, II. 2018. Urban forests form isolated archipelagos. *Journal of Urban Ecology* **4**(1).

Pinheiro J, Bates D, DebRoy S, Sarkar D, Team RC 2021. nlme: Linear and Nonlinear Mixed Effect Models.

Pretzsch H, Biber P, Uhl E, Dahlhausen J, Schütze G, Perkins D, Rötzer T, Caldentey J, Koike T, Con Tv, et al. 2017. Climate change accelerates growth of urban trees in metropolises worldwide. *Scientific Reports* **7**(1): 15403.

R Development Core Team version 4.1.1 2020. R: A Language and Environment for Statistical Computing. Vienna, Austria: R Foundation for Statistical Computing.

Roye D, Sera F, Tobias A, Lowe R, Gasparrini A, Pascal M, de'Donato F, Nunes B, Teixeira JP. 2021. Effects of Hot Nights on Mortality in Southern Europe. *Epidemiology* **32**(4): 487-498.

Sanusi R, Johnstone D, May P, Livesley SJ. 2017. Microclimate benefits that different street tree species provide to sidewalk pedestrians relate to differences in Plant Area Index. *Landscape and Urban Planning* **157**: 502-511.

Saunders SC, Chen J, Drummer TD, Crow TR. 1999. Modeling temperature gradients across edges over time in a managed landscape. *Forest Ecology and Management* **117**(1): 17-31.

Schmidt M, Jochheim H, Kersebaum K-C, Lischeid G, Nendel C. 2017. Gradients of microclimate, carbon and nitrogen in transition zones of fragmented landscapes – a review. *Agricultural and Forest Meteorology* **232**: 659-671.

Schwaab J, Meier R, Mussetti G, Seneviratne S, Bürgi C, Davin EL. 2021. The role of urban trees in reducing land surface temperatures in European cities. *Nature Communications* **12**(1): 6763.

Seco R, Karl T, Guenther A, Hosman KP, Pallardy SG, Gu L, Geron C, Harley P, Kim S. 2015. Ecosystem-scale volatile organic compound fluxes during an extreme drought in a broadleaf temperate forest of the Missouri Ozarks (central USA). *Global Change Biology* **21**(10): 3657-3674.

Smith JG, Sconiers W, Spasojevic MJ, Ashton IW, Suding KN. 2012. Phenological Changes in Alpine Plants in Response to Increased Snowpack, Temperature, and Nitrogen. *Arctic, Antarctic, and Alpine Research* **44**(1): 135-142.

Smoyer KE, Rainham DGC, Hewko JN. 2000. Heat-stress-related mortality in five cities in Southern Ontario: 1980–1996. *International Journal of Biometeorology* **44**(4): 190-197.

Sodoudi S, Zhang H, Chi X, Müller F, Li H. 2018. The influence of spatial configuration of green areas on microclimate and thermal comfort. *Urban Forestry & Urban Greening* **34**: 85-96.

Şöhretoğlu D, Renda G. 2020. The polyphenolic profile of Oak (Quercus) species: a phytochemical and pharmacological overview. *Phytochemistry Reviews* **19**(6): 1379-1426.

Sonti NF, Hallett RA, Griffin KL, Sullivan JH. 2019. White oak and red maple tree ring analysis reveals enhanced productivity in urban forest patches. *Forest Ecology and Management* **453**: 117626.

Stewart ID, Oke TR. 2012. Local climate zones for urban temperature studies. *Bulletin of the American Meteorological Society* **93**(12): 1879-1900.

UN. 2019. World Urbanization Prospects: The 2018 Revision (ST/ESA/SER.A/420). New York: United Nations, Departement of Economic and Social Affairs Population Division

van den Bosch M, Ode Sang Å. 2017. Urban natural environments as nature-based solutions for improved public health – A systematic review of reviews. *Environmental Research* **158**: 373-384.

van Hove LWA, Jacobs CMJ, Heusinkveld BG, Elbers JA, van Driel BL, Holtslag AAM. 2015. Temporal and spatial variability of urban heat island and thermal comfort within the Rotterdam agglomeration. *Building and Environment* **83**: 91-103.

Vasenev V, Varentsov M, Konstantinov P, Romzaykina O, Kanareykina I, Dvornikov Y, Manukyan V. 2021. Projecting urban heat island effect on the spatial-temporal variation of microbial respiration in urban soils of Moscow megalopolis. *Science of the Total Environment* **786**.

Verhelst TE, Vangansbeke P, De Frenne P, D'hont B, Ponette Q, Willems L, Verbeeck H, Calders K. 2023. Forest edge structure from terrestrial laser scanning to explain bird biophony characteristics from acoustic indices. *Remote Sensing in Ecology and Conservation* **n/a**(n/a).

Verheyen K, Baeten L, De Frenne P, Bernhardt-Romermann M, Brunet J, Cornelis J, Decocq G, Dierschke H, Eriksson O, Hedl R, et al. 2012. Driving factors behind the eutrophication signal in understorey plant communities of deciduous temperate forests. *Journal of Ecology* **100**(2): 352-365.

von Arx G, Pannatier EG, Thimonier A, Rebetez M. 2013. Microclimate in forests with varying leaf area index and soil moisture: potential implications for seedling establishment in a changing climate. *Journal of Ecology* **101**(5): 1201-1213.

Wang X, Dallimer M, Scott CE, Shi W, Gao J. 2021. Tree species richness and diversity predicts the magnitude of urban heat island mitigation effects of greenspaces. *Science of the Total Environment* **770**: 145211.

Wang Y, Akbari H. 2016. The effects of street tree planting on Urban Heat Island mitigation in Montreal. *Sustainable Cities and Society* **27**: 122-128.

Winbourne JB, Jones TS, Garvey SM, Harrison JL, Wang L, Li D, Templer PH, Hutyra LR. 2020. Tree Transpiration and Urban Temperatures: Current Understanding, Implications, and Future Research Directions. *Bioscience* **70**(7): 576-588.

WMO. 2008. Guide to Meteorological Instruments and Methods of Observation, Appendix 4B. WMO-N. 8 (CIMO Guide). Geneva.

Yan H, Wu F, Dong L. 2018. Influence of a large urban park on the local urban thermal environment. *Science of the Total Environment* **622-623**: 882-891.

Zellweger F, Coomes D, Lenoir J, Depauw L, Maes SL, Wulf M, Kirby KJ, Brunet J, Kopecky M, Malis F, et al. 2019. Seasonal drivers of understorey temperature buffering in temperate deciduous forests across Europe. *Global Ecology and Biogeography* **28**(12): 1774-1786.

Zhu S, Yang Y, Yan Y, Causone F, Jin X, Zhou X, Shi X. 2022. An evidence-based framework for designing urban green infrastructure morphology to reduce urban building energy use in a hot-humid climate. *Building and Environment* **219**: 109181.

Zipper SC, Schatz J, Singh A, Kucharik CJ, Townsend PA, Loheide SP. 2016. Urban heat island impacts on plant phenology: intra-urban variability and response to land cover. *Environmental Research Letters* **11**(5): 054023.

Ziter CD, Pedersen EJ, Kucharik CJ, Turner MG. 2019. Scale-dependent interactions between tree canopy cover and impervious surfaces reduce daytime urban heat during summer. *Proceedings of the National Academy of Sciences of the United States of America* **116**(15): 7575-7580.

Zuur AF, Ieno EN, Smith GM. 2009. *Mixed effects models and extensions in ecology with* R. New York: Springer.